ELSEVIER

Journal of Nuclear Materials 258–263 (1998) 339–344

journal of nuclear materials

Neutron radiation effects of the center conductor post in a low aspect ratio tokamak reactor

Yican Wu *, Bingjia Xiao, Qunying Huang, Lijian Qiu

Institute of Plasma Physics, Academia Sinica, P. O. Box 1126, Hefei, Anhui 230031, People's Republic of China

Abstract

The fully exposed CCP in a low aspect ratio tokamak will receive high neutron damage, electrical resistive heating and neutron heating, which is one of the key components of the reactor and requires replacement at regular intervals. This paper gives the analysis results for the CCP in the low aspect ratio transmutation reactor considering parameters such as nuclear heating deposit, thermal-hydraulics parameters, radiation damage etc. Finally, those results are compared with those for the first wall of conventional tokamaks assuming the same technical requirements.

1. Introduction

Low aspect ratio tokamaks (CT: compact tori, spherical tori) with aspect ratio (A) in the range of 1.2–2.0 offer the possibilities of compact volumetric fusion neutron sources as well as fusion reactors requiring relatively low external fields [1,2]. Furthermore, this kind of compact tokamak might offer some attractive advantages such as a cost-effective, high performance (high stable beta in the first stability boundary) plasma regime [3]. It could be used economically and safely to the transmutation of long-lived actinides and fission products [4]. Recent progress [5–7] in tokamak physics theory and experiment provide added impetus to the verification of the physics in this regime and the assessment of its reactor prospects.

A design with an aspect ratio near the lower limit (due to limited space) requires an unshielded center conductor post (CCP) as part of the toroidal field coil (TFC) circuit. The fully exposed CCP will receive severe neutron damage, resistive and nuclear heating power, which is one of the key components with high power density and high irradiation damage and requires replacement at regular intervals. This paper gave the analysis results for the CCP considering neutron radiation effects in the low aspect ratio tokamak reactor comparing with those estimated for the first wall (FW) of regular tokamak reactors (RT) to show if the technical requirements are comparable. A reference design of the compact tokamak reactor and the calculational models for investigating neutron radiation effects in the CCP were given in Section 2. The neutron wall loading and nuclear heating distributed in the CCP and the first wall were calculated with MCNP/3B [8] based on 3-D geometrical configurations and presented in Sections 3 and 4. The removal of resistive heating and nuclear heating in the CCP was considered and calculated with the THPBHR [9] based on a 2-D cylindrical geometrical model in Section 5. The values of dpa-per-full-power-year in the CCP and first wall were calculated with the 1-D neutron transport code ANISN [10] and compared with those for regular tokamak reactors in Section 6. Finally the analysis results were concluded in Section 7.

2. Reference reactor and computational model

As a reference design, the overview of the compact tokamak transmutation reactor [4] is given in Fig. 1. A set of possible design parameters are indicated in Table 1.

As depicted in Fig. 2(a), the simplified 3-D calculational model with the lower aspect ratio limit of 1.2 requires a CCP made from copper with the radius of 0.2 m.

* Corresponding author. Tel.: +86 551 5591310; fax: +86 551 5591397; e-mail: ycwu@ipnc1.hfcas.ac.cn.

0022-3115/98/$19.00
PII: S0022-3115(98)00365-1

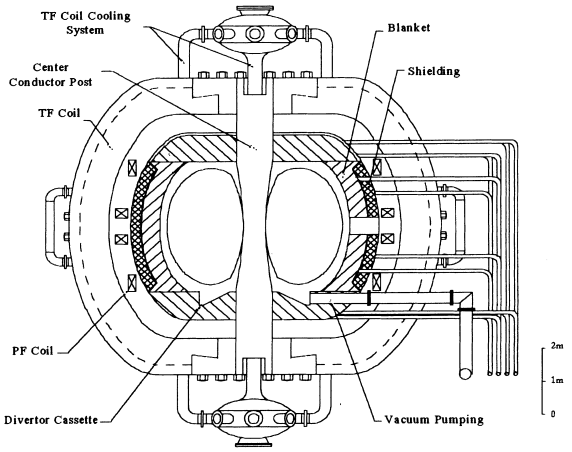

Fig. 1. Overview of Hefei low aspect ratio transmuter.

The sizes and relevant parameters are listed in Table 2 and material compositions are listed in Table 3. A set of reference design parameters for the conventional tokamak reactor are given in Table 2 for the purpose of comparison calculation. The overview of the corresponding 3-D calculational model is depicted in Fig. 2(b).

Table 1
Parameters of Hefei low aspect ratio transmuter

Major radius R [m]	1.2
Minor radius a [m]	1
Plasma current I_p [MA]	13
Toroidal field B_t [T]	1.6
Plasma edge q	7.7
Average density$\langle n_e \rangle$ [10^{20} m^{-3}]	0.8
Average temperature$\langle T \rangle$[keV]	9
Plasma volume [m^3]	43
Bootstrap current fraction	0.5
Fusion power P_{fu}[MW]	60
Drive power P_d[MW]	40
Neutron wall loading [MWm^{-2}]	0.7

For convenient comparison, the same plasma profiles (''neutron source zone'' with half-round-cross-section shown in Fig. 2) are used in the calculation. A homogeneous and isotropic neutron source is assumed.

3. Neutron wall loading distribution

The 3-D Monte-Carlo neutron photon transport code MCNP/3B [8] were used to calculate the poloidal

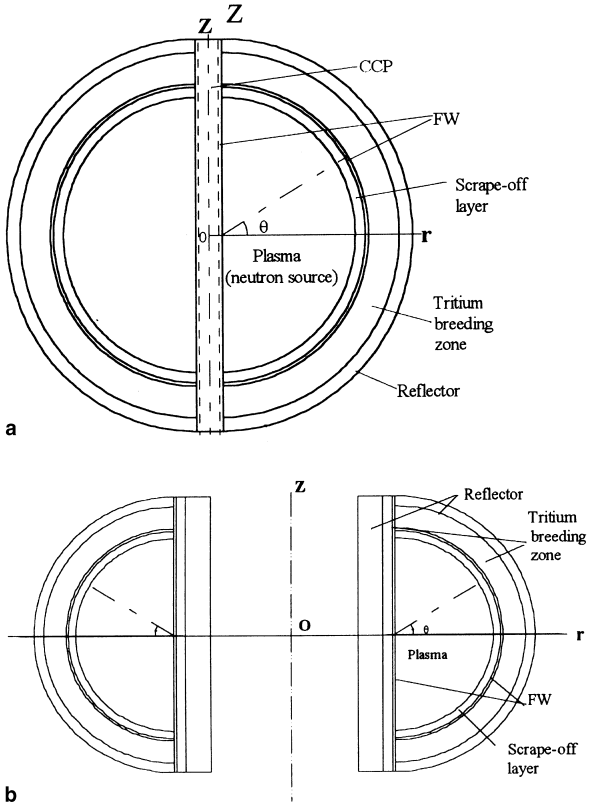

Fig. 2. (a) 3-D computational model of the compact torus. (b) 3-D computational model of the regular torus.

Table 2
The main parameters of reference designs

Reference design	Compact torus	Regular tokamak
Major radius R (m)	1.2	4
Aspect ratio A	1.2	4
Inner scrape-off layer (m)	0	0
Outer scrape-off layer (m)	0.15	0.15
Radius of CCP (m)	0.2	/
Depth of first wall (m)	0.01	0.01
Depth of tritium	0.5	0.5 (outer)
Breeding zone		0.2 (inner)
Depth of reflector (m)	0.2	0.2 (outer)
		0.5 (inner)

distribution of neutron wall loading P_w on the surface of the CCP and the FW for the CT as well as the RT. The results were normalized to an average neutron wall load ($\overline{P}_w$) of 1 MW/m^2 on the whole exposed surface.

Fig. 3(a) and (b) showed that peak wall loading on the FW and the CCP along poloidal direction (θ) and axial direction (Z) is lower than that calculated for the regular tokamak. Table 4 showed that the average value of P_w on the CCP is lower than that on the outer F of CT (compact tokamak), and also lower than that of inner and outer FW of RT (regular tokamak).

Table 3
Material compositions and volume fractions

Zone	Material compositions and volume fractions
Plasma zone	void
Scrape-off layer	void
First wall	Cu: 100%
Tritium breeding zone	Be: 55% + Li_2O:20% + He-gas: 25%
Reflector	C: 100%

Table 4
The average value of P_w (MW/m^2)

Zone	Outer FW	Inner FW
CT	1.02	0.72 [a]
RT	1.08	0.81

[a] For the surface of the exposed CCP.

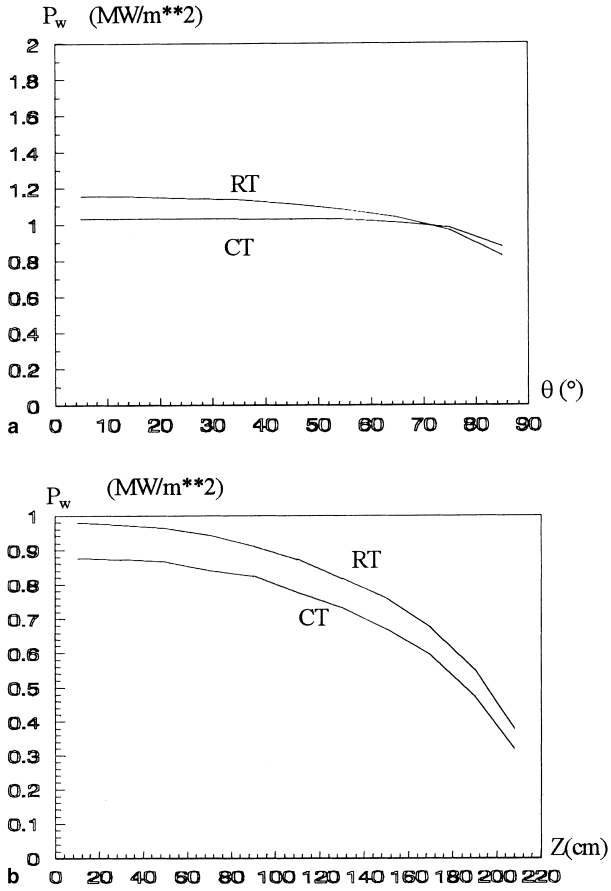

Fig. 3. (a) Poloidal distribution of P_w in the outer FW. (b) Axial distribution of P_w on the inner FW.

4. Nuclear heating distribution

The spatial distribution of nuclear heating density (H_n) in the CCP and the FW were calculated with the 3-D Monte-Carlo neutron photon transport code MCNP/3B and relevant pointwise cross-section data library [8]. The results were normalized to an average neutron wall load ($\overline{P}_w$) of 1 MW/m^2 on the whole exposed surface (FW).

The nuclear heating distributions were given in Fig. 4(a) for the outer FW along poloidal direction (θ), in Fig. 4(b) for the inner FW (referring to the 1-cm-thick surface layer of the CCP for the CT) along axial direction (Z) and in Fig. 4(c) for the CCP along the radial direction (r), respectively. The results showed that nuclear heating density in the outer FW of the CT is lower than that of the RT, but nuclear heating density in the CCP (inner FW) of the CT is higher than that in the outer FW of the RT, which is the reversed trend to the distribution of neutron wall loading and explained by the fact that the exposed CCP can be more easily penetrated by the neutrons emitted from the toroidal plasma zone in comparison with the case of the RT with a larger size of inner shielding blanket. Therefore, the removal of nuclear heating and radiation damage of material in the CCP should be studied seriously. It can be noted that the maximum nuclear heating density exists at the midplane of the CCP. The average nuclear heating density of the CCP is 4.35 W/cm^3 when normalized to an average neutron wall loading ($\overline{P}_w$) of 1 MW/m^2 (see Table 5).

Table 5
The average value of H_n (W/cm^3)

Zone	Whole CCP	Outer FW	Inner FW
CT	4.35	7.26	6.39 [a]
RT	/	8.28	5.72

[a] For the 1-cm-thick surface layer of the CCP.

5. Heat removal and thermal-hydraulic analysis

The CCP is cooled by pressurized water flowing vertically through coolant channels uniformly distributed in the CCP. Thermal-hydraulic calculation was carried out by the modified 2-D THPBHR code which was developed to analyze the thermal-hydraulics of first

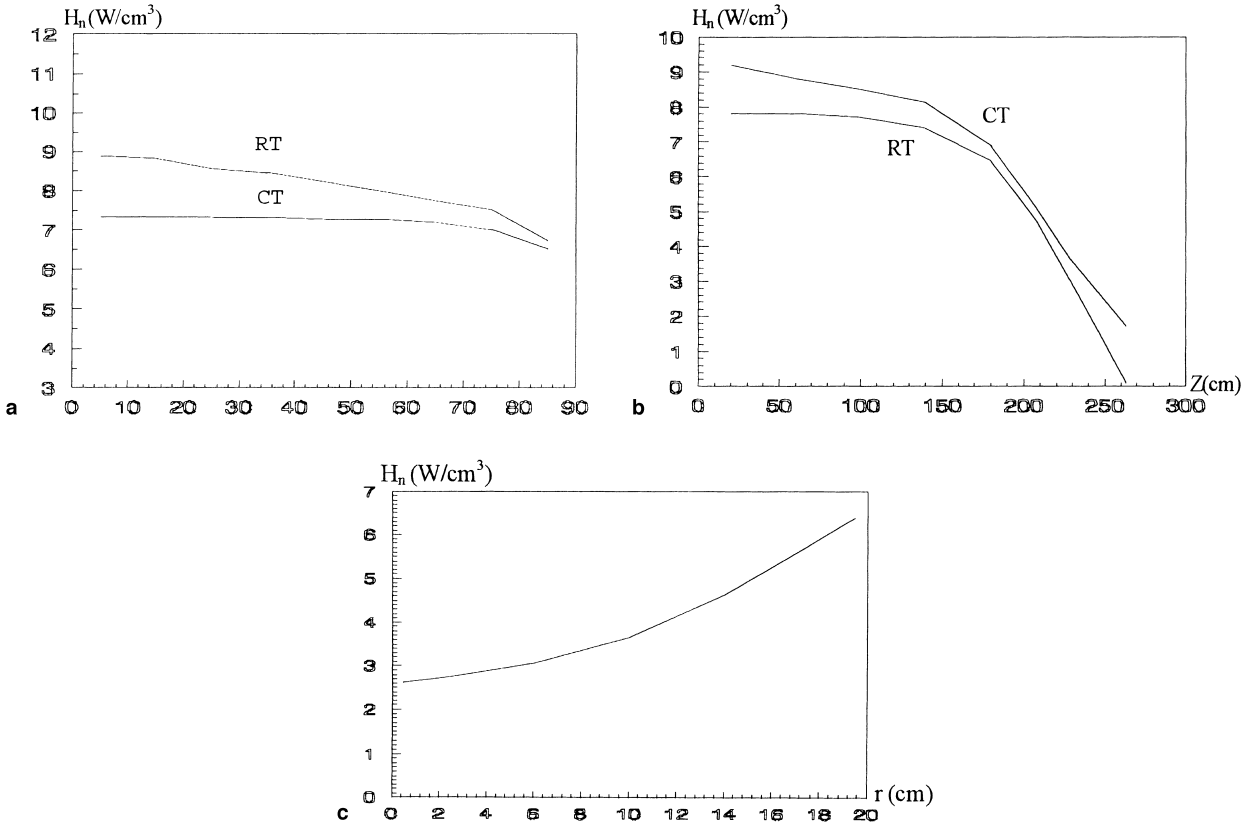

Fig. 4. (a) Poloidal distribution of H_n in the outer FW. (b) Axial distribution of H_n in the inner FW. (c) Radial distribution of H_n in the CCP.

wall and pebble-bed blanket of hybrid reactor or fusion reactor concepts [9].

Axisymmetric geometry was used to model the CCP with coolant channels, i.e. the CCP is simplified as a layer-by-layer concentric cylindrical shells of copper and coolant. Radial and axial variations of nuclear heating in the CCP were considered in calculation. The variation in electrical resistivity of copper with temperature was also taken into account. Because the variations of thermo-physical properties of copper and water are relatively minor in the temperature range of interest, they were ignored. As described in the previous section, the nuclear heating deposition in the CCP was calculated with MCNP/3B.

The reference design parameters of the CCP and the thermal-hydraulic calculation results were given in Table 6. It was shown that the maximum copper temperature (362 K) is far lower than 573 K threshold for significant swelling [13]. Therefore, the nuclear heating and resistive dissipation heating can be effectively removed with appropriate heat removal design.

Table 6
Thermal-hydraulic design parameters

Material of the CCP	Copper
Current through the CCP, I_c (MA)	4.94 [a]
Radius of the CCP, R_c (m)	0.2
Length of the CCP (m)	4.30
Current density, J_c (kA/cm^2)	5.31
Neutron wall loading, P_w (MW/m^2)	4.5 [b]
Radius of coolant channel (m)	0.005
Coolant	Water
Coolant volume fraction	26%
Coolant velocity (m/s)	6.1
Coolant pressure drop (bar)	5.0
Pump power (kW)	14.1
Inlet coolant temperature (K)	323
Outlet coolant temperature (K)	351
Peak copper temperature (K)	362
Nuclear heating (MW)	10.3
Resistive dissipation heating (MW)	22.6

[a] According to the formula [11]:

$$I_c/I_p \approx 2q_\psi \left(\frac{\pi}{2\kappa}\right)^2 (A-1)^2,$$

where I_p – Plasma current (13 MA), q_ψ – average edge safety factor (7.7), A – aspect ratio (1.2) and κ – plasma elongation to the divertor x-point (2.0) [12].

[b] Given by Ref. [12].

6. Radiation damage

Radiation transport calculation was carried out to estimate the displacement per atom (dpa) in CCP and FW with the 1-D discrete ordinates transport code ANISN [10] and the 25-group neutron, 21-group gamma coupled cross section library UW [14]. A spherical geometry model was used to represent the CCP and blanket assemblies of the CT. A toroidal cylindrical geometry model was used to represent the inboard and outboard blanket-shield assemblies of the RT to account for the toroidal distribution of neutrons in the plasma region. The machine center was taken as the geometrical center of each model.

The values of the dpa-per-full-power-year in the CCP and the FW were summarized in Table 7. The results were normalized to an average neutron wall load of 1 MW/m^2. In addition, the values of the dpa-per-full-power-year in the FW of ITER [15] and UWMAK-I [16] were given for comparison. Table 7 showed that the damage severity for the CCP of compact tokamak and FW of conventional tokamaks do not significantly differ in the dpa-values on the basis of a normalized neutron wall load of 1 MW/m^2. However, radiation damage of the CCP is still worth being considered seriously, particularly when a high $\overline{P}_w$ exists because the average values of dpa in the whole CCP were not much lower than those for the FWs of compact and regular tokamaks.

7. Conclusion

3-D neutron wall loading and nuclear heating distribution calculation, 2-D heat removal calculation and 1-D neutron radiation damage calculation have been performed to assess the engineering feasibility of the unshielded CCP of a low aspect ratio tokamak reactor. The analyses above have shown that:

The severity of neutron radiation damage is comparable, or a little lower than, with that estimated for the first wall of conventional tokamak reactors on the basis of the same average neutron wall loading of 1 MW/m^2.

Table 7
Comparison of dpa-per-full-power-year for various reference reactors

Ref. reactor and component	CT			RT		UWMAK-I	ITER	
	Whole CCP	Inner FW [a]	Outer FW	Inner FW	Outer FW	FW	FW	
Materials	Cu	Cu	Cu	Cu	Cu	316ss	316ss	Cu
dpa/year [b]	8.7	12.2	14.0	15.5	18.0	18	9.3	10.1

[a] 1-cm-thick surface layer of CCP.

[b] Normalized to an average neutron wall load of 1 MW/m^2.

However, radiation damage and other relevant problems of the CCP need to be studied further since a high average dpa can be expected in the whole CCP, especially with a high neutron wall loading.

The nuclear heating deposited and resistive dissipation heat can be effectively removed to ensure that the maximum copper temperature is far below the 523 K threshold for significant swelling.

Additional studies on other engineering and technology problems of the CCP such as demountable construction, stress analysis, radiation transmutation effects on electrical conductivities, etc. are needed before such reactors can be seriously considered.

References

[1] Y.-K.M. Peng, D.J. Strickler, Nucl. Fusion 26 (1986) 769.
[2] Y.-K.M. Peng, J.B. Hicks, Engineering Feasibility of Tight Aspect Ratio Tokamak (spherical torus) Reactors, presented at the Symposium on Fusion Technology, 1990, London.
[3] L.J. Qiu, Z.J. Guo, Y.C. Wu et al., Some key issues of compact tokamak reactor design for volumetric neutrin source (VNS) application, The Third Sino-Japanese Symposium on Materials for Advanced Energy Systems and Fission and Fusion Engineering, Chengdu, People's Republic of China, 1995.
[4] J. Qiu, Z. Guo, B.J. Xiao et al., A low aspect ratio tokamak transmutation reactor, presented at the Fourth International Symposium on Fusion Nuclear Technology (ISFNT-4), Tokyo, Japan, April 6–11, 1997.
[5] JET TEAM, Plasma Physics Cont. Nucl. Fusion Res. 1988 1 (1989) 41.
[6] E.A. Lazarus et al., Cont. Fusion and Plasma Heating, vol. 14B, Part I (EPS, 1990) 427.
[7] M. Kikuchi et al., Nucl. Fusion 30 (1990) 343.
[8] MCNP/3B Monte Carlo Neutron and Photon Tansport Code Collection, CCC-200 (1989).
[9] B.J. Xiao, L.J. Qiu, Steady state thermal-hydraulic models of pebble bed blanket on hybrid reactors, Fusion Eng. and Design 27 (1995) 253–257.
[10] W.W. Engle, A User's Manual for ANISN, USAEC Report K-1693, 1967.
[11] Y.S. Hwang et al., Exploration of Low aspect Ratio Tokamak Regimes in CDX-U and TS-3 Devices, Seville, Spain, 26 September – 1 October 1994/IAEA-CN-60/A5-II-6.
[12] Qiang Xu, Shaojie Wang, Alpha Particle Transport in Low Aspect Ratio Tokamak Reactor, The Third Sino-Japanese Symposium on Materials for Advanced Energy Systems and Fission and Fusion Engineering, Chengdu, People's Republic of China, 30 October – 3 November 1995.
[13] H.R. Brager, F.A. Garner, in: N.H. Packan et al. (Eds.), Effects of Radiation on Materials, ASTM-STP 1046 (1990) 599.
[14] R.T. Perry, G.A. Moses, A Combined P_3 Vitamin-C, Macklib-IV, Coupled 25 Neutron-21 Gamma Group Cross Section Library – The UW Cross Section Library, UWFDM-390, University of Wisconsin, 1980.
[15] Detail of the ITER Outline Design Report, ITER-TAC-4-07, for ITER TAC Meeting No. 4, 10–12 January 1994, presented by the ITER director.
[16] M.A. Abdou, R.W. Conn, Nucl. Sci. Eng. 55 (1974) 256–266.